FEBS 22670 FEBS Letters 459 (1999) 177–185

Function of the second nucleotide-binding fold in the CFTR chloride channel

Bryan Zerhusen, Jianjie Ma*

Department of Physiology and Biophysics, Case Western Reserve University School of Medicine, 10900 Euclid Avenue, Cleveland, OH 44106, USA

Received 5 August 1999

Abstract To test the role of nucleotide-binding fold (NBF) 2 and its interaction with the regulatory (R) domain in the function of the cystic fibrosis transmembrane conductance regulator (CFTR) channel, we used three deletion mutants of CFTR: ΔR(708-835), ΔNBF2(1185-1349) and ΔR-ΔNBF2. In lipid bilayers, ΔNBF2 channel activity is ATP- and cAMP-dependent protein kinase (PKA)-dependent, but unlike wild-type (wt) CFTR, it displays a reduced activity and insensitivity to 5′-adenylylimidodiphosphate (AMP-PNP). Both ΔR and ΔR-ΔNBF2 channels are PKA-independent, but ΔR activity is reduced whereas ΔR-ΔNBF2 activity is increased. Deletion of NBF2 from CFTR affects protein trafficking and channel gating kinetics. The data suggest that NBF2 could have inhibitory and stimulatory roles in CFTR activity by interaction with NBF1 directly or indirectly via the R domain.

Key words: Cystic fibrosis; HEK 293 cell; Single channel recording; Phosphorylation

1. Introduction

The cystic fibrosis transmembrane conductance regulator (CFTR) belongs to the family of ATP-binding cassette transporters [1,2], which contain two transmembrane domains and two nucleotide-binding folds (NBF1 and NBF2). Unique to CFTR is a large intracellular regulatory (R) domain that contains multiple consensus cAMP-dependent protein kinase (PKA) phosphorylation sites [3,4]. CFTR is a chloride channel whose activity is controlled by PKA phosphorylation of serine residues in the R domain [4–7] and ATP-binding and hydrolysis at the NBFs [8,9]. The dual regulatory mechanism of the CFTR channel by intracellular ATP and PKA requires coordinated interactions between the NBFs and the R domain. Previous studies show that partial deletion of the R domain from CFTR, ΔR(708-835), leads to an ATP-dependent and PKA-independent chloride channel with a significantly lower open probability than that of the wild-type (wt) CFTR channel [10–12]. It is possible that deletion of the R domain removes both inhibitory and stimulatory effects conferred by the R domain on the CFTR chloride channel function. Addition of exogenous unphosphorylated R domain protein (amino acids 588–858) to wt-CFTR blocks the chloride channel activity [13], suggesting that the unphosphorylated R domain is inhibitory. Conversely, exogenous phosphorylated R domain protein (amino acids 588–858 or 645–834) stimulated the ΔR channel, suggesting that the phosphorylated R domain is stimulatory [11,12].

The first and second NBFs of CFTR share sequence similarity in certain conserved regions, but the overall amino acid similarity between the two NBFs of CFTR is only ~30%. Mutations of the corresponding residues in the Walker A and Walker B motifs in NBF1 and NBF2 have different effects on the function of the CFTR channel [14–18]. In NBF1, mutation of the conserved lysine (Walker A) or aspartate (Walker B) residues results in a decreased channel activity, whereas comparable mutations in NBF2 cause an increase in channel bursting durations.

To further study the function of NBF2 and its possible interactions with the R domain in the regulation of the CFTR channel, we created three deletion mutants of CFTR: ΔR(708-835), ΔNBF2(1185-1349) and ΔR-ΔNBF2. These mutant CFTR proteins were expressed in HEK 293 cells and their chloride channel functions were examined using the lipid bilayer reconstitution technique. Our rationale is as follows. If ATP hydrolysis at NBF2 functions simply to close the CFTR channel as proposed by Carson et al. [16], then, deletion of NBF2 would cause an increase in CFTR channel activity. Hwang et al. [9] proposed that in a fully phosphorylated CFTR channel, binding of ATP (or 5′-adenylylimidodiphosphate (AMP-PNP)) at NBF2 stabilizes the open state and the hydrolysis of ATP at NBF2 leads to termination of a burst of open events. According to this model, deletion of NBF2 may result in a decrease in the channel open probability (P_o), possibly due to altered interaction of the phosphorylated R domain and NBF1. Such effects would be reflected in the altered ATP-dependent gating of the ΔNBF2 and ΔR-ΔNBF2 channels. In a different study, Gunderson and Kopito [18] proposed that ATP-binding and hydrolysis at NBF2 is important for the open-closed transitions and the stabilization of conductance states of the CFTR channel. As such, one would predict that deletion of NBF2 would completely eliminate channel activity. Our single channel measurements showed that the ΔNBF2 channel had reduced open lifetimes and a reduced open probability compared with the wt-CFTR channel, whereas the ΔR-ΔNBF2 channel exhibited prolonged open durations and an increased open probability compared with the wt-CFTR channel. These data present functional evidence of the interaction of NBF2 with the R domain and provide new insights into the gating mechanisms of the CFTR channel.

*Corresponding author. Fax: (216) 368-1693.
E-mail: jxm63@po.cwru.edu

Abbreviations: CFTR, cystic fibrosis transmembrane conductance regulator; PKA, cAMP-dependent protein kinase; PM, plasma membrane; NBF, nucleotide-binding fold; AMP-PNP, 5′-adenylylimidodiphosphate; pS, picosiemen; DPC, diphenylamine-2-carboxylate

PII: S0014-5793(99)01230-2

2. Materials and methods

2.1. Subcloning of the CFTR gene

The CFTR cDNA contains two restriction sites for the *Msc*I restriction enzyme at nucleotide positions 3554 and 4046. Digestion of pBluescript(wt-CFTR) with *Msc*I results in deletion of a 492 bp cDNA fragment from CFTR, which encodes amino acids 1185–1349. The deleted amino acids correspond to majority of the NBF2 region and thus was named pBluescript(ΔNBF2). Previously, the wt-CFTR cDNA and the ΔR(708-835) CFTR mutant have been cloned into the pCEP4 eukaryotic expression vector [19,13]. The pCEP4(ΔNBF2) construct was generated by substituting the wt cDNA in pCEP4(wt-CFTR) with the corresponding cDNA fragment from pBluescript(ΔNBF2) between the *Bst*1107I and *Xho*I restriction sites. Similarly, the pCEP4(ΔR-ΔNBF2) mutant was generated by replacing the *Bst*1107I-*Xho*I fragment from pCEP4(ΔR-CFTR) with that from pBluescript(ΔNBF2).

2.2. Expression of CFTR in HEK 293 cells

A human embryonic kidney cell line (293-EBNA, Invitrogen) was used for transfection and expression of wt and mutant CFTR proteins. The culture conditions for maintaining the HEK 293 cells were as described previously [20,21]. The parental cell line was grown to confluence in a 37°C incubator with 5% CO_2 and passaged 1:5, 2 days before gene transfer. pCEP4(WT), pCEP4(ΔR), pCEP4(ΔNBF2) or pCEP4(ΔR-ΔNBF2) was introduced into HEK 293 cells, using lipofectamine reagent (Gibco BRL). Two days after transfection, the cells were used for a Western blot assay or isolation of membrane vesicles followed by reconstitution studies in the lipid bilayer membranes.

2.3. Isolation of microsomal membrane vesicles

HEK 293 cells expressing the wt-, ΔR-, ΔNBF2- or ΔR-ΔNBF2-CFTR proteins were harvested and microsome membranes were isolated with a combination of hypotonic lysis, Dounce homogenization and differential centrifugation as described in Xie et al. [20].

2.4. Reconstitution of the CFTR chloride channel

Lipid bilayer membranes were formed across an aperture of ~200 μm diameter with a lipid mixture of PS:PE:cholesterol of 6:6:1. The lipids are dissolved in decane to a concentration of 40 mg/ml [21]. The recording solutions are as follows: *cis* (intracellular): 200 mM CsCl, 2 mM Mg-ATP, 10 mM HEPES-Tris (pH 7.4) and *trans* (extracellular): 50 mM CsCl, 10 mM HEPES-Tris (pH 7.4). ATP and AMP-PNP solutions are prepared in 100 mM HEPES-Tris (pH 7.4) and stored in 100 μl aliquots at −80°C until use. Microsomal vesicles containing either wt-, ΔR-, ΔNBF2- or ΔR-ΔNBF2-CFTR proteins were added to the *cis* solution. To study the PKA-dependent regulation of the CFTR channel, 50 U/ml of the catalytic subunit of PKA was added to the *cis* solution. All experiments are performed at room temperature (~22–25°C).

Single channel currents were recorded using an Axopatch 200A patch clamp unit (Axon Instruments). Data acquisition and pulse generation were performed with a 486 computer and a 1200 Digidata A/D-D/A converter. The currents were sampled at 2.5 ms/point and filtered at 100 Hz. Single channel analyses were performed with pClamp7 software (Axon Instruments). All recordings are measured by delivering a 5 s pulse from a holding potential of 0 mV. Figs. 2, 4 and 7 show consecutive 5 s pulses plotted head to tail.

2.5. Criteria for establishing stable CFTR channel activity in the lipid bilayer

The CFTR channels incorporated into the lipid bilayer are defined

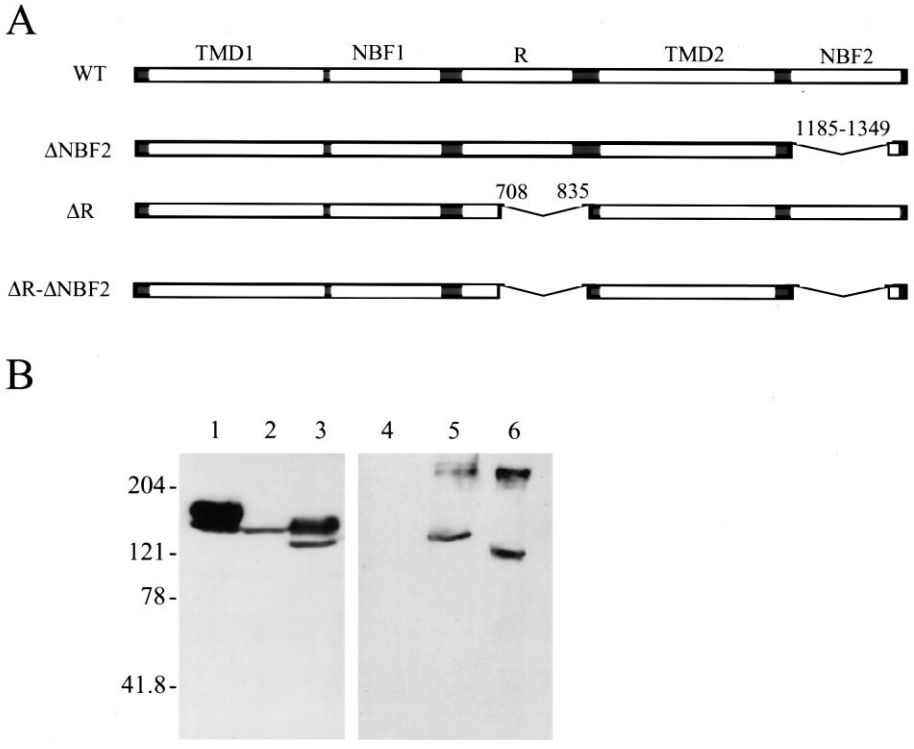

Fig. 1. Expression of CFTR in HEK 293 cells. A: Schematic representation of the CFTR deletion mutants. Regions deleted in the R domain correspond to amino acids 708–835, while amino acids 1185–1349 are removed from NBF2. B: HEK 293 cells transfected with pCEP4(wt), pCEP4(ΔF508), pCEP4(ΔR), pCEP4(ΔNBF2) or pCEP4(ΔR-ΔNBF2) were lysed with RIPA buffer and whole cell lysate was used in a Western blot. The proteins were separated on a 3–12% SDS-polyacrylamide gel and probed with a monoclonal antibody mAb24-1 directed against the C-terminal portion of CFTR (Genzyme). Each lane represents approximately the same number of cells grown on a 100 mm dish. Proteins were visualized by exposure to Kodak X-Omat AR film for 1 min. wt-CFTR (lane 1), ΔF508 (lane 2), ΔR (lane 3), untransfected HEK 293 cells (lane 4), ΔNBF2 (lane 5), ΔR-ΔNBF2 (lane 6). The high molecular weight band present in lanes 5 and 6 (~300 kDa) is likely due to aggregation of the CFTR molecules. Similar aggregations of wt-, ΔR- and ΔF508-CFTR proteins were also observed when the protein samples were heated at 75°C for over 20 min.

according to several criteria: specifically, ATP-dependence, anion selectivity, linear current-voltage relationship and sensitivity to block by diphenylamine-2-carboxylate (DPC). The frequency of acquiring a CFTR channel in the bilayer membrane depended on the efficiency of the transient transfection, which varied slightly from preparation to preparation. For every vesicle preparation, Western blot was always performed to confirm the CFTR expression in these cells.

Closed-time histograms and open-time histograms are constructed with a cutoff of 2.5 ms, which is the rate of digitization. Bilayers with multiple CFTR channels were excluded from the data analysis. The closed-burst duration histograms (Figs. 4 and 7) are created with a cutoff which excludes closed durations shorter than 60 ms. The open probability is determined by measuring the fractional time that the channel spends in the open state. To prevent CFTR channel 'rundown', we have taken the following measures. First, 100 U of PKA is present in the *cis* solution to maintain optimal phosphorylation of the channel. Second, our previous studies show that the microsomal vesicles do not appear to contain phosphatase activities, as addition of PKI does not result in rundown of CFTR channels [11]. Third, we routinely used a 'diary plot' of P_o versus time to illustrate an effect of substrates added to the CFTR channel [13,11,22].

3. Results

3.1. Expression and subcellular localization of CFTR proteins in HEK 293 cells

The ΔNBF2 construct was generated through deletion of 164 amino acids (amino acids 1185–1349) from CFTR, which correspond to the major portion of NBF2. The ΔR-ΔNBF2 construct is a double deletion mutant of CFTR which lacks amino acid residues 708–835 and 1185–1349 (Fig. 1A). These deletion mutants, along with ΔF508, ΔR(708-835) and wt-CFTR, were transiently expressed in HEK 293 cells using the liposome-based DNA transfection method [11,13]. HEK 293 cells transfected with pCEP4(wt-CFTR) expressed fully glycosylated CFTR protein with a molecular weight of ∼170 kDa, plus some core-glycosylated CFTR proteins (∼140 kDa) (Fig. 1B, lane 1). Cells transfected with pCEP4(ΔF508) expressed only the core-glycosylated form of CFTR with a molecular weight of ∼140 kDa (Fig. 1B, lane 2). The corresponding full- and core-glycosylated CFTR proteins with the ΔR mutant run at a molecular weight of ∼150 and ∼120 kDa, respectively (Fig. 1B, lane 3), reflecting the deletion of 128 amino acids from the R domain. Cells transfected with pCEP4(ΔNBF2) and pCEP4(ΔR-ΔNBF2) exhibit bands at ∼120 and ∼110 kDa, respectively (Fig. 1B, lanes 5 and 6). The sizes of the ΔNBF2 and ΔR-ΔNBF2 proteins are consistent with the core-glycosylated forms. However, a higher molecular weight band of ∼120 kDa could be detected with ΔR-ΔNBF2 after a longer exposure of the gel (data not shown).

3.2. Lipid bilayer reconstitution of ΔNBF2 and ΔR-ΔNBF2 channels

To test whether ΔNBF2 and ΔR-ΔNBF2 proteins are functional, microsomal membrane vesicles were isolated from HEK 293 cells transfected with pCEP4(ΔNBF2) and pCEP4(ΔR-ΔNBF2). The vesicles containing either the ΔNBF2 or ΔR-ΔNBF2 proteins were incorporated into the lipid bilayer membrane for measurement of single CFTR channel activities and their functions were compared with those of the wt and ΔR channels (Fig. 2).

Similar to the wt-CFTR channel (Fig. 2A), the ΔNBF2 forms a functional chloride channel in the lipid bilayer whose openings strictly depended on the presence of ATP and PKA in the intracellular solution (Fig. 2C). Previously, we have demonstrated that the reversal potential for the endogenous CFTR from T84 cells and wt-CFTR expressed in HEK 293 cells is +22.4 mV [23]. Under an asymmetric ionic condition of 200 mM CsCl (*cis*)/50 mM CsCl (*trans*), the current-voltage relationship for ΔNBF2 had an extrapolated reversal potential of +28.6 ± 18.0 mV (see Fig. 5C), indicative of the anion selective feature of the ΔNBF2 channel. The large S.E.M. of the reversal potential is due to the lack of data points at positive potentials. The wt-CFTR channel has a slope conductance of 8.2 ± 0.6 picosiemen (pS) [23], while the ΔNBF2 channel has a slope conductance of 6.1 ± 1.5 pS. The activity of the ΔNBF2 channel could be completely blocked by 3 mM DPC added to the extracellular solution (not shown), which is a characteristic feature of the CFTR channel. With 2 mM ATP and 50 U/ml of PKA present in the *cis* intracellular solution, the ΔNBF2 channel had an average open probability (P_o) of 0.062 ± 0.019 ($n = 11$) at a −80 mV test potential. This P_o is ∼5-fold lower than that of the wt-CFTR channel under similar experimental conditions [13]. Thus, deletion of NBF2 from CFTR results in an ATP- and PKA-dependent chloride channel with a reduced open probability compared with that of the wt-CFTR channel.

The ΔR-ΔNBF2 proteins also formed functional chloride channels in the bilayer membrane (Fig. 2D). Similar to the wt-CFTR and ΔNBF2 channels, opening of the ΔR-ΔNBF2

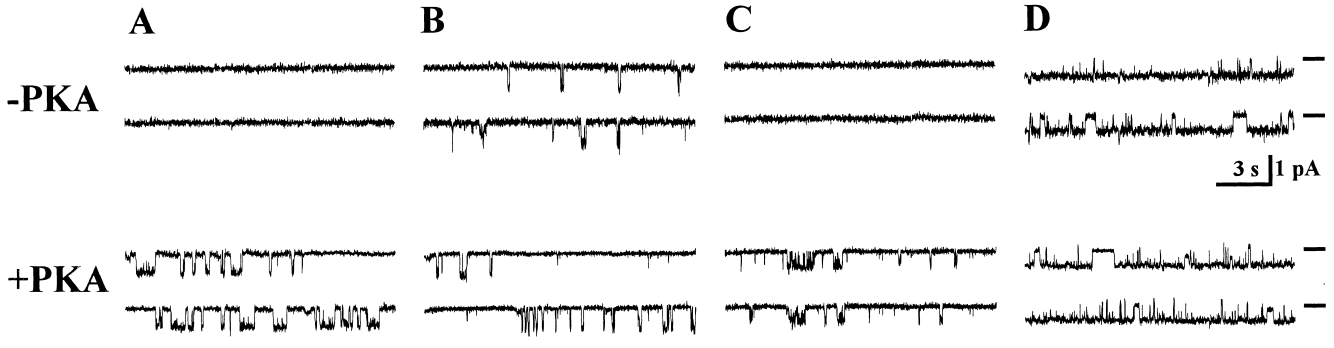

Fig. 2. PKA-dependence of CFTR channels. Traces are taken from a single channel incorporated into the lipid bilayer, at a test potential of −80 mV. The recording solutions contained: 200 mM CsCl, 10 mM HEPES (pH 7.2), 1 mM $MgCl_2$ and 2 mM ATP in the *cis* (intracellular) chamber and 50 mM CsCl and 10 mM HEPES (pH 7.2) in the *trans* (extracellular) chamber. Vesicles containing CFTR proteins were added to the *cis* solution. The top traces show activity of a single CFTR channel in the absence of PKA (−PKA). The bottom traces show channels after the addition of PKA (+PKA). (A) wt-CFTR, (B) ΔR, (C) ΔNBF2, (D) ΔR-ΔNBF2.

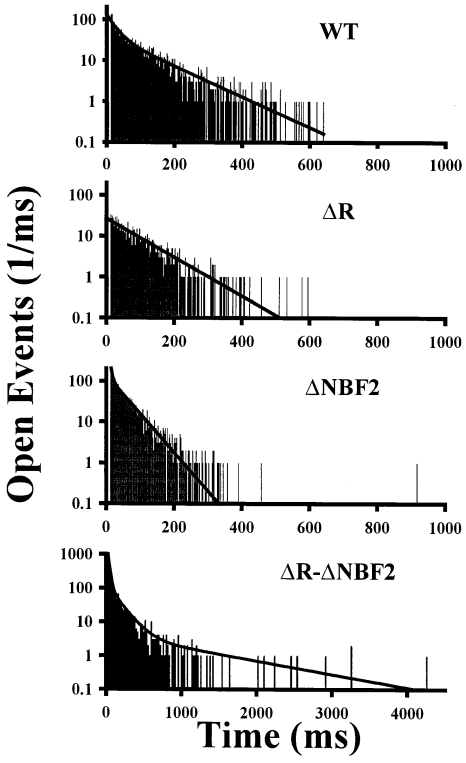

Fig. 3. Open-time histograms of wt, ΔR, ΔNBF2 and ΔR-ΔNBF2 channels. Open-time histograms were constructed at a test potential of −80 mV, with total open events of 2403, 946, 2148 and 1156 for wt, ΔR, ΔNBF2 and ΔR-ΔNBF2 channels, respectively. The solid lines represent the best fits using the Simplex-Least Squares (SLS) fitting routines (pStat program of pClamp7 software) (SLS values = 3.6–9.4), according to $y = y_{o1}/\tau_{o1}\ \exp(-t/\tau_{o1}) + y_{o2}/\tau_{o2}\ \exp(-t/\tau_{o2})$, where $y_{o1} = 1181$, $\tau_{o1} = 24.3$ ms, $y_{o2} = 1943$, $\tau_{o2} = 248.8$ ms (wt); $y_{o1} = 2470$, $\tau_{o1} = 91.9$ ms (ΔR); $y_{o1} = 9690$, $\tau_{o1} = 5.7$ ms, $y_{o2} = 6378$, $\tau_{o2} = 46.0$ ms (ΔNBF2). The histogram for the ΔR-ΔNBF2 channel was fitted with three exponential terms, with $y_{o1} = 66\,123$, $\tau_{o1} = 20.5$ ms, $y_{o2} = 19\,574$, $\tau_{o2} = 140.0$ ms, $y_{o3} = 4291$, $\tau_{o3} = 1096.6$ ms.

channel also required the hydrolysis of intracellular ATP, as AMP-PNP (2 mM) alone was insufficient to induce channel openings ($n = 9$). Similar to the ΔR channel, opening of the ΔR-ΔNBF2 channel was completely independent of PKA phosphorylation, i.e. the mutant CFTR channels lacking the R domain opened in the absence of PKA and its activity did not change upon PKA phosphorylation (Fig. 2B,D). Different from the ΔR channel, the ΔR-ΔNBF2 channel exhibited prolonged open states, with an average open probability of 0.529 ± 0.053 ($n = 11$), while the average P_o of the ΔR channel was 0.122 ± 0.012 [11].

3.3. Gating kinetics of the wt, ΔR, ΔNBF2 and ΔR-ΔNBF2 channels

Visual inspection of the single channel records shown in Fig. 2 reveals different gating kinetics of the ΔNBF2 and ΔR-ΔNBF2 channels compared to those of the wt-CFTR and ΔR channels. The open lifetimes of the ΔNBF2 channel appear to be shorter than those of the wt-CFTR and the open lifetimes of the ΔR-ΔNBF2 channel appear to be longer than those of the wt-CFTR and ΔR channels. These differences are characterized in the analyses of the open-time histograms shown in Fig. 3. The wt-CFTR channel has two open states with time constants of $\tau_{o1} = 24$ ms and $\tau_{o2} = 248$ ms, respectively, and the ΔR channel has one open state with a time constant of 92 ms. These values are similar to our previously published data [11,20,23]. The open-time histogram of the ΔNBF2 channel contained two exponential components with time constants of $\tau_{o1} = 6$ ms and $\tau_{o2} = 46$ ms, which are significantly smaller than those of the wt-CFTR channel. The ΔR-ΔNBF2 channel contained a long open state, $\tau_{o3} = 1096$ ms, plus two open states with values similar to those of the wt-CFTR ($\tau_{o1} = 20$ ms, $\tau_{o2} = 140$ ms).

To further delineate the gating kinetics of the CFTR mutants, the closed-time histograms were generated with the wt-CFTR, ΔR, ΔNBF2 and ΔR-ΔNBF2 channels (Fig. 4). Fig.

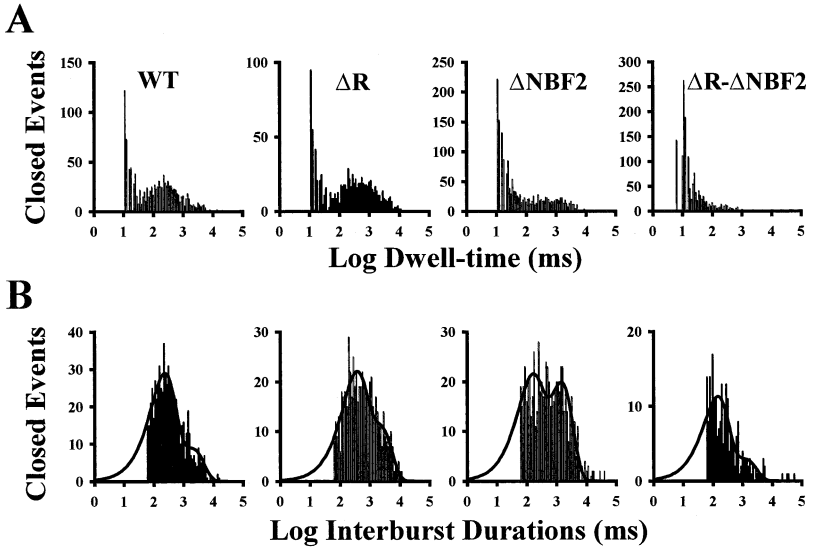

Fig. 4. Closed-time histogram of wt, ΔR, ΔNBF2 and ΔR-ΔNBF2 channels. The closed-time histograms were constructed from the same sets of data presented in (A). The data were binned on a logarithmic scale. The histograms shown in (B) represent the closed-burst durations, with a delimiter set at $\tau_c = 60$ ms. The solid lines represent the fits with the lowest SLS values (2.1–10.6) according to $y = P_2\ \exp(t-\alpha_2-\exp(t-\alpha_2)) + P_3\ \exp(t-\alpha_3-\exp(t-\alpha_3))$, where $\alpha_2 = \log(\tau_2)$ and $\alpha_3 = \log(\tau_3)$ and P_2 and P_3 represent the proportion of the channel occurring in the τ_2 and τ_3 states, respectively. The best fit parameters are, $P_2 = 0.75$, $\tau_2 = 216$ ms, $P_3 = 0.25$, $\tau_3 = 1889$ ms (wt); $P_2 = 0.62$, $\tau_2 = 310$ ms, $P_3 = 0.38$, $\tau_3 = 2092$ ms (ΔR); $P_2 = 0.45$, $\tau_2 = 128$ ms, $P_3 = 0.55$, $\tau_3 = 1412$ ms (ΔNBF2); $P_2 = 0.78$, $\tau_2 = 136$ ms, $P_3 = 0.22$, $\tau_3 = 1154$ ms (ΔR-ΔNBF2).

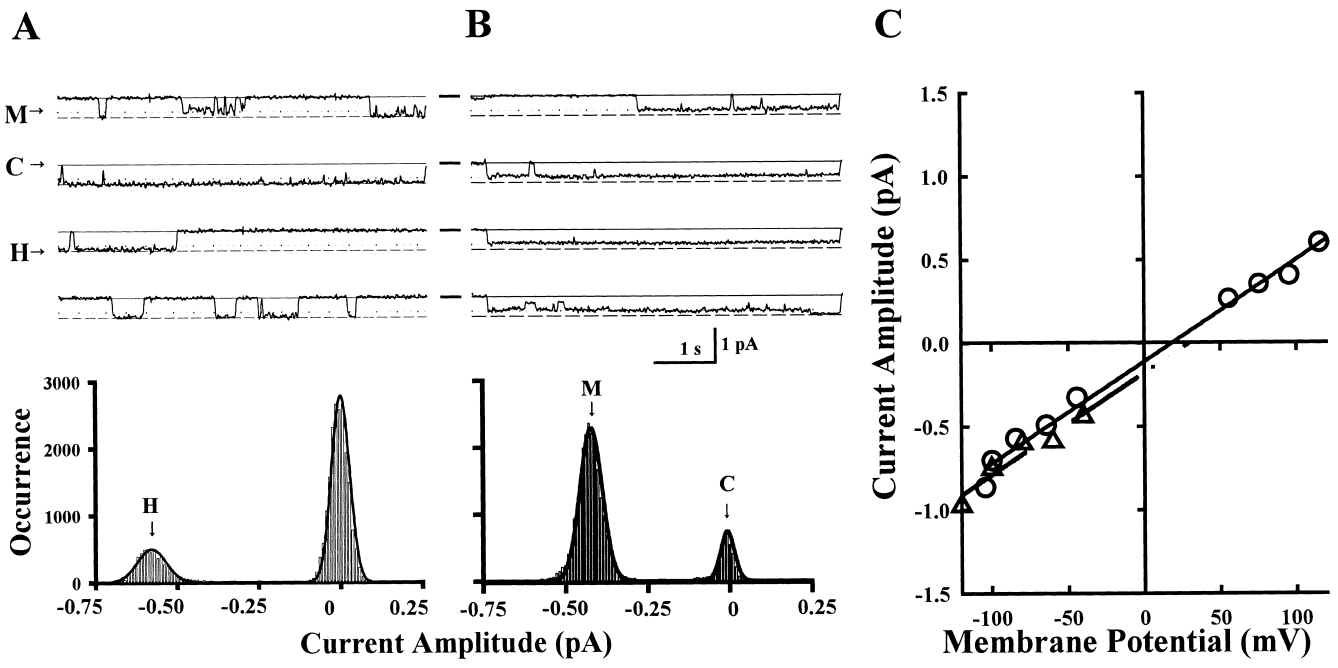

Fig. 5. Subconductance state of the ΔR-ΔNBF2. Representative single channel currents from wt-CFTR (A) or ΔR-ΔNBF2 (B) channels were obtained at a test potential of −65 mV. H represents the full conductance state and M represents the subconductance state. Panels at the bottom were all-point current amplitude histograms for the wt-CFTR (left) and the ΔR-ΔNBF2 channel (right). The solid lines represent the best fit Gaussian distribution with a mean current amplitude of 0.598 ± 0.025 pA (wt-CFTR) and 0.452 ± 0.040 pA (ΔR-ΔNBF2). The current-voltage relationships of the ΔNBF2 (Δ, short dashes) and ΔR-ΔNBF2 (○, solid line) channels are shown in C. The ΔNBF2 channel had a slope conductance of 6.1 ± 1.5 pS and a reversal potential of +28.6 ± 18.0 mV. The ΔR-ΔNBF2 channel had a slope conductance of 6.0 ± 0.2 pS and a reversal potential of +15.8 ± 2.9 mV.

4A plots the closed events as a function of the logarithmic time. All histograms contained a fast component in addition to several slow components. The fast component (τ_{c1}) had a time constant of approximately 20 ms, which is similar in all four CFTR channels. This 20 ms closed state probably represents the fast closing events within an open-burst of the CFTR channel, as reported earlier [16]. To facilitate identification of the slow closing components of the CFTR channels, a delimiter of $\tau_c = 60$ ms was set to construct the closed-burst duration histograms [16,17]. The 60 ms represents the nadir between the fast and slow components of the histograms shown in Fig. 4A. As shown in Fig. 4B, all closed-burst duration histograms could be adequately fit with two exponential components. The intermediate closed state (τ_{c2}) had time constants ranging from 128 to 310 ms and the long closed state (τ_{c3}) had time constants ranging from 1347 to 2092 ms. Although the values of τ_{c2} and τ_{c3} were similar among the four CFTR channels, the relative occurrence of τ_{c3} over τ_{c2} differed significantly between the wt-CFTR and the three CFTR mutants. For the wt-CFTR channel, the τ_{c3} state represents 0.25 of the closed-burst events. However, the τ_{c3} state for the ΔR, ΔNBF2 and ΔR-ΔNBF2 channels corresponds to 0.38, 0.43 and 0.22 of the closed-burst events, respectively.

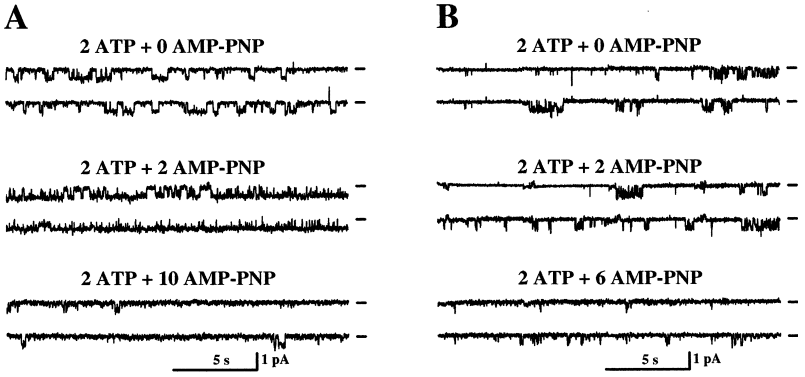

Fig. 6. Effects of AMP-PNP on wt-CFTR and ΔNBF2 channels. Records shown are taken from the same experiment with either a single wt-CFTR (A) or the ΔNBF2 (B) channel incorporated into the bilayer. Under conditions of 2 mM ATP (top), the ΔNBF2 channel had an average $P_o = 0.062 \pm 0.019$ and the wt-CFTR channel had $P_o = 0.226 \pm 0.035$. After the addition of 2 mM AMP-PNP (middle), P_o of the ΔNBF2 channel did not change (0.058 ± 0.023), but P_o of the wt-CFTR channel increased to 0.459 ± 0.079. Further addition of 6 mM AMP-PNP to ΔNBF2 (bottom right) reduced the activity of the channel to $P_o = 0.008 \pm 0.001$, while the P_o of wt-CFTR was reduced to 0.103 ± 0.018 at 10 mM AMP-PNP (bottom left).

3.4. Subconductance states of the ΔR-NBF2 channel

Deletion of NBF2 from CFTR also affects the distribution of conductance states of the chloride channels. Fig. 5 shows representative single channel currents from the wt-CFTR (Fig. 5A) and ΔR-ΔNBF2 channel (Fig. 5B) at a test potential of −65 mV. To facilitate identification of the open current amplitude, the single channel records were digitally filtered at 20 Hz. Here, the open current level of the substate was labelled as M and that of the full open state was labelled as H. From the current-amplitude histogram analyses, the wt-CFTR channel had a single channel current of 0.598 ± 0.025 pA, whereas the ΔR-ΔNBF2 channel had a single channel current of 0.452 ± 0.040 pA. The corresponding current-voltage relationship for the ΔR-ΔNBF2 channel had a slope conductance of 6.0 ± 0.2 pS (Fig. 5C, ○), which was ~20% smaller than that of the wt-CFTR channel [23]. Interestingly, the conductance state of the ΔR-ΔNBF2 channel is similar to one of the subconductance states of the wt-CFTR channel, namely the intermediate state (M) observed in our previous studies [23]. The M state only exists as a transition state in the wt-CFTR channel, but it is the dominant conductance state in the ΔR-ΔNBF2 channel (Fig. 5A,B).

3.5. ATP-dependent gating of the wt and ΔNBF2 channel

To study the role of ATP hydrolysis in the function of the ΔNBF2 channel, two sets of experiments were performed. First, we tested the effect of increasing concentrations of AMP-PNP on the gating of the wt-CFTR and the ΔNBF2 channels (Fig. 6). Under control conditions with 2 mM ATP and 50 U/ml of PKA present in the intracellular solution, the wt-CFTR channel had an open probability of 0.226 ± 0.035 (Fig. 6A, top), while the ΔNBF2 channel had an average open probability of 0.062 ± 0.019 (Fig. 6B, top). Following the addition of 2 mM AMP-PNP, the P_o of the wt-CFTR channel increased to 0.459 ± 0.079 ($n = 16$) (Fig. 6A, middle), whereas the activity of the ΔNBF2 channel remained unchanged ($P_o = 0.058 \pm 0.023$, $n = 5$) (Fig. 6B, middle). The wt-CFTR channels did not display a decrease in activity or inhibition until the concentration of AMP-PNP was increased to 10 mM. After the addition of AMP-PNP to 10 mM, the open probability of the wt-CFTR channel was decreased to 0.103 ± 0.018 ($n = 4$) (Fig. 6A, bottom), compared to the P_o of the ΔNBF2 channel which was reduced to essentially zero ($P_o = 0.008 \pm 0.001$, $n = 3$) at 6 mM AMP-PNP (Fig. 6B, bottom).

AMP-PNP, which is a poorly hydrolyzable analog of ATP, presumably would interfere with ATP-binding and hydrolysis at the NBFs and thereby alter the CFTR gating properties. Based on studies with the wt-CFTR channel, it has been proposed that AMP-PNP at the intermediate concentrations (1–5 mM) interacts preferentially with NBF2 and thus increases the open duration of the wt-CFTR channel [9,16,18,24]. The lack of a stimulatory effect of AMP-PNP on the ΔNBF2 channel and the fact that AMP-PNP can inhibit the activity of the

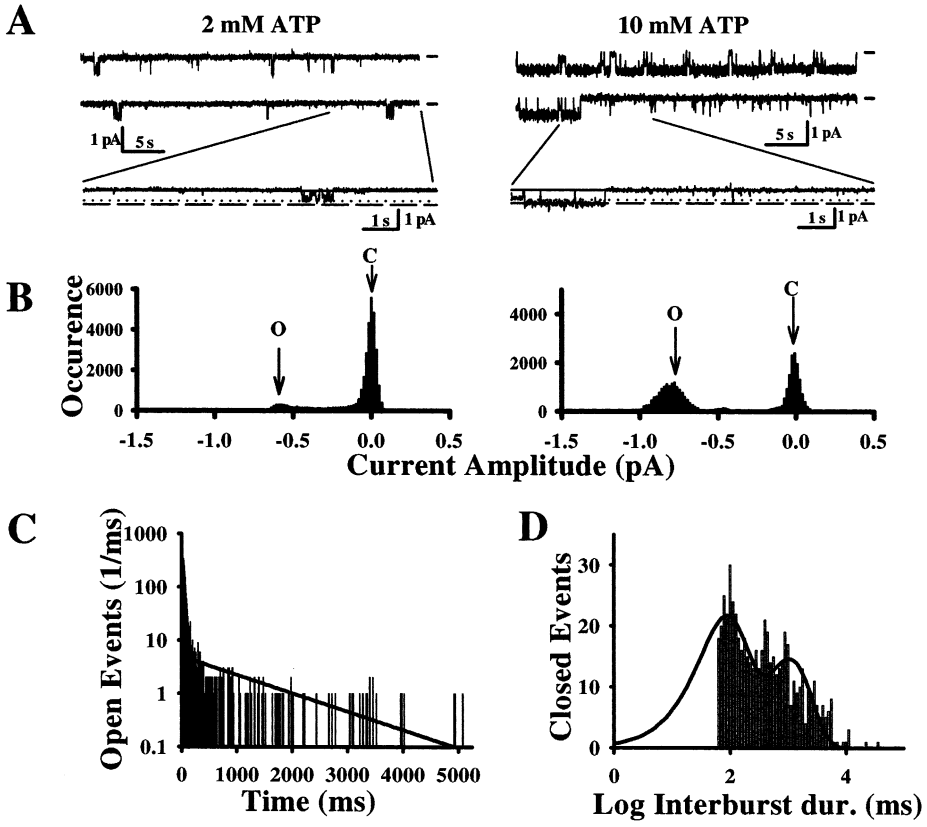

Fig. 7. Effect of ATP on the ΔNBF2 channel. Representative single channel currents were taken from the ΔNBF2 channel incorporated into the bilayer under conditions of 2 mM ATP (left) or 10 mM ATP (right) present in the *cis* cytosolic solution (A). The corresponding all-point current amplitude histograms are shown in (B). The histograms shown in (C) represent the open-times (SLS value = 4.7) (left) and (D) interburst durations (right) (SLS value = 3.6) of the ΔNBF2 channel at 10 mM ATP. The open histogram contained two exponential components with time constants of $\tau_{o1} = 27.0$ ms, $\tau_{o2} = 1263.3$ ms. With a delimiter set at $\tau_c = 60$ ms, the closed-burst durations contained two exponential components, with $P_2 = 0.57$, $\tau_2 = 76$ ms, $P_3 = 0.43$, $\tau_3 = 1029.8$ ms (see Fig. 5 for definition).

ΔNBF2 channel suggest that ATP hydrolysis at NBF1 plays a key role in opening of the wt-CFTR channel.

Next, we compared the effect of increasing concentrations of ATP on the activity of the ΔNBF2 and wt-CFTR channels (Fig. 7). With 10 mM ATP present in the cytosolic solution (*cis*), P_o of the ΔNBF2 channel was approximately 5-fold higher ($P_o = 0.290 \pm 0.110$, $n = 10$) compared with the corresponding value at 2 mM ATP (Fig. 7). The increase in P_o was accompanied by an additional increase in single channel conductance as indicated by the leftward shift in the current amplitude histogram (Fig. 7B). As indicated by the representative traces in Fig. 7, transitions to the substates still exist but are less frequent at 10 mM ATP. The enhanced P_o of the ΔNBF2 channel at 10 mM ATP was mainly a result of increases in open lifetimes of the channel (Fig. 7C, $\tau_{o1} = 27$ ms and $\tau_{o2} = 1263$ ms). The closed-time constants of the ΔNBF2 channel at 10 mM ATP were comparable to those at 2 mM ATP (Fig. 7D).

4. Discussion

In this study, we examined the function of three CFTR deletion mutants, ΔR, ΔNBF2 and ΔR-ΔNBF2. We expressed these mutants, as well as wt-CFTR and ΔF508, in HEK 293 cells. While the wt-CFTR appears as both fully glycosylated and core-glycosylated in HEK 293 cells, the ΔNBF2 and ΔR-ΔNBF2 constructs are expressed in the core-glycosylated form, resembling ΔF508. The Western blot data indicate that ΔNBF2, ΔR-ΔNBF2 and ΔF508 are processing mutants. The use of green fluorescent protein fusion constructs confirms that the ΔNBF2 and ΔR-ΔNBF2 proteins are likely retained in the endoplasmic reticulum membrane of HEK 293 cells (data not shown). Interestingly, it appeared that at least some of the ΔR-ΔNBF2 proteins could be fully glycosylated. When reconstituted into the lipid bilayer membrane, both ΔNBF2 and ΔR-ΔNBF2 form functional chloride channels. Opening of the ΔNBF2 channel required both ATP hydrolysis and PKA phosphorylation, while activity of the ΔR and the ΔR-ΔNBF2 channels was PKA-independent.

4.1. Comparison with previous studies

Although the ΔNBF2 proteins are retained in intracellular membranes, they are capable of forming functional chloride channels. Our findings that ΔNBF2 and ΔR-ΔNBF2 can form functional chloride channels are in contrast to an earlier study by Rich et al. [26], who concluded that CFTR lacking NBF2 (amino acids 1157–1414) reached the plasma membrane (PM) of HeLa cells but lacked a chloride transport function determined with the 6-methoxy-*N*-(3-sulfopropyl)quinolinium assay. However, using the microsomal membrane vesicles isolated from HEK 293 cells containing the ΔNBF2 proteins, we consistently detected ATP- and PKA-dependent chloride channels in the lipid bilayer membrane. Our study differs from that of Rich et al. [26] in the actual CFTR constructs (our ΔNBF2 lacks amino acids 1185–1349 and their ΔNBF2 lacks amino acids 1157–1414) and in the expression systems used (HeLa versus HEK 293 cells), which may account for the different results.

One potential caveat of studying the NBF2 deletion mutant of CFTR is the possible changes in the global conformation of the mutant CFTR proteins. Indeed, the ΔNBF2 mutant not only exhibits altered gating kinetics, but is also defective in trafficking as the ΔNBF2 proteins are retained in the intracellular membranes. In addition, the conductance state of the ΔNBF2 channel also appears to be reduced (at 2 mM ATP) compared with that of the wt-CFTR channel (Fig. 7). Studies from other investigators have identified a complicated process associated with the biosynthetic pathway of CFTR, such that less than 20% of the nascent CFTR molecules can be properly processed and trafficked to the PMs [27]. Mutations in different regions of CFTR, either changes in single amino acids, i.e. ΔF508 and P574H [17], or regional deletions, i.e. Δexon5 and Δ19 [20,28], all lead to difficulty in proper folding and have a significant impact on the processing of CFTR proteins. However, electrophysiological measurements have shown that these mis-processed CFTR proteins can maintain functional chloride channel activities, either in the intracellular membranes [20,28,29] or when rescued to the PM [30,17]. ΔNBF2, a processing mutant of CFTR, is capable of functioning as a chloride channel and is strictly regulated by ATP and PKA. The ΔNBF2 channel is selective for chloride over cesium ions and is sensitive to inhibition by DPC. The low P_o of the ΔNBF2 channel is not an artifact of protein processing, as a previous study showed that the Δ19 processing mutant has gating characteristics and an open probability similar to the wt-CFTR [20]. Instead, the reduced activity of the ΔNBF2 channel probably reflects the altered ATP-dependent gating of CFTR (Fig. 7). These results suggest that with the deletion of NBF2, the overall conformation of CFTR proteins is largely intact.

The wt-CFTR channel has two subconductance states of ~6 pS (M, intermediate) and 2.7 pS (L, low) in addition to the full conductance state (~8 pS, H, high) [23,28]. These three conductance states (H, M and L) interconvert with slow kinetics [23]. The ΔR-ΔNBF2 and ΔNBF2 channels remain open stably in the M state, a state previously observed less than 2% of the time in wt-CFTR [23]. Interestingly, the subconductance state of the ΔNBF2 channel increases to the full open state in the presence of 10 mM ATP (Fig. 7). At present, we do not understand the molecular mechanism behind the subconductance states of the CFTR channel. Gunderson and Kopito [18] also observed two conductance states with the wt-CFTR, a full open state (O2) plus a substate (O1) with a conductance that is about 15% smaller than that of the O2 state. The conductance state of the ΔNBF2 channel resembles the O1 state reported by Gunderson and Kopito [18].

4.2. Single channel properties of ΔNBF2, ΔR and ΔR-ΔNBF2

The gating kinetics of the ΔNBF2 channel are different from the wt-CFTR channel. The open lifetimes of the ΔNBF2 channel are shorter than those of the wt-CFTR channel (Fig. 3), suggesting that the closing rates of the chloride channel are increased as a result of deleting the NBF2 region. The closed-time histogram of the ΔNBF2 channel exhibits a different distribution from that of the wt channel. The longer closed events occur more frequently in the ΔNBF2 channel than in the wt-CFTR channel (Fig. 4). Thus, it is likely that the rate of channel opening to a burst state is also altered in the ΔNBF2 channel. These combined changes result in an overall 5-fold reduction in open probability of the ΔNBF2 channel. Unlike the wt-CFTR channel, both ΔR and ΔNBF2 channels are insensitive to stimulation by AMP-PNP. The stimulatory effect of AMP-PNP on the wt-CFTR channel has been interpreted as the preferential interaction of

AMP-PNP with NBF2 [16]. Thus, it is not surprising to see that the ΔNBF2 channel lacks this stimulatory response since it presumably lacks the binding site for AMP-PNP. On the other hand, the lack of a stimulatory effect of AMP-PNP on the ΔR channel would suggest that removal of the R domain causes possible changes in the function of NBF2 [11]. This may also indicate that the effect of AMP-PNP in the wt-CFTR channel may be mediated by the R domain. Interestingly, AMP-PNP at higher concentrations causes inhibition of both wt-CFTR, ΔR and ΔNBF2 channels, which probably reflects the competition of AMP-PNP with ATP at NBF1 for binding and/or hydrolysis.

Opening of the ΔR-ΔNBF2 channel is independent of PKA phosphorylation, with a P_o that is significantly higher than that of the wt-CFTR channel. This is in contrast to the low P_o of both ΔR and ΔNBF2 channels. Thus, it appears that the mutant CFTR channel lacking either the R domain (amino acids 708–835) or NBF2 (amino acids 1185–1349) alone has reduced functional activities, whereas double deletion of the R domain and NBF2 leads to an increase in the channel activities. The apparent low open probability of the ΔNBF2 and ΔR channels and the high open probability of the ΔR-ΔNBF2 channel suggest that NBF2 could have both stimulatory and inhibitory roles in the overall function of CFTR, possibly through interaction with the R domain and/or NBF1.

4.3. Implications for CFTR channel functions

CFTR forms a chloride channel in which parts of the transmembrane domains constitute the pore for chloride ions. The R domain functions as a channel inhibitor until it is phosphorylated by PKA and undergoes a conformational change that initiates channel activity. Phosphorylation of the R domain may have two effects on CFTR, the first could be permissive, releasing a steric hindrance on the channel, the second might be stimulatory, facilitating interaction of ATP with the NBFs [9,25,31,32]. Once the R domain is phosphorylated, hydrolysis of ATP takes place at NBF1, which leads to opening of the chloride channel. Stabilization of the open state could then be mediated through an interaction of NBF2 with the phosphorylated R domain [9]. Subsequent hydrolysis of ATP at NBF2 may then close the channel [9,16]. The data presented here with the ΔNBF2, ΔR and ΔR-ΔNBF2 channels suggest that the gating of the CFTR channel involves a coordinated interaction among the three cytosolic domains of CFTR: NBF1, R and NBF2.

From our previous studies and work from other investigators, we know that the R domain contains both stimulatory and inhibitory regions that mediate the function of the CFTR channel [11–13,25,33]. PKA phosphorylation of serine residues in the R domain of wt-CFTR either removes the inhibitory or enhances the stimulatory interactions between the R domain and NBF1, allowing for ATP hydrolysis to occur at NBF1, leading to opening of the CFTR channel. In a mechanism similar to that proposed by Hwang et al. [9], the open-burst state of the wt-CFTR may be prolonged because NBF2 interacts with the inhibitory region of the R domain and prevents the channel from entering the closing state. Hydrolysis of ATP at NBF2 would alter the interaction between NBF2 and R and allow for both R domain and NBF2 to interact with NBF1, causing fast channel closings from the open-burst state.

To explain the altered gating kinetics and overall functions of the ΔNBF2, ΔR and ΔR-ΔNBF2 channels, we propose that NBF2, in addition to the inhibitory effect (via ATP hydrolysis to terminate the bursting state of the wt-CFTR channel), also has a stimulatory role in the function of the CFTR channel by serving as an auxiliary site for the inhibitory region of the R domain. The dual inhibitory effects of the R domain and NBF2 explain how a channel lacking either the R domain (ΔR) or NBF2 (ΔNBF2) can both exhibit a reduced P_o. Additionally, the low P_o and insensitivity of the ΔR channel to AMP-PNP may suggest that the R domain is required for the normal ATP-binding/hydrolysis at NBF2. The ΔR channel presumably lacks the inhibitory region of the R domain, since it opens without requiring PKA phosphorylation. In the absence of this inhibitory region, NBF2 can exert a direct inhibitory effect on NBF1 and thus lead to a reduction in P_o of the ΔR channel. The lack of AMP-PNP activation on the ΔR channel can be explained by assuming that the inhibitory effect of NBF2 on NBF1 can occur independently of ATP hydrolysis at NBF2. In the absence of NBF2, there is no docking site for the inhibitory region of the R domain and the balance will shift to the inhibition of ATP hydrolysis at NBF1 by the inhibitory region of the R domain. Therefore, the bursting kinetics of the ΔNBF2 channel will be interrupted by frequent brief closings, accounting for the low P_o of the ΔNBF2 channel. The ΔR-ΔNBF2 channel lacks both the R domain and NBF2, which presumably lacks both negative regulatory functions of CFTR, and thus would exhibit elevated channel activities. In this case, channel opening, presumably through ATP hydrolysis at NBF1, occurs independently of PKA phosphorylation and is free of the inhibitory effects of NBF2 and the R domain.

One would predict that a mutation in NBF2 that enhances the interaction with the inhibitory region of the R domain or reduces the inhibitory interaction with NBF1 should lead to an increase in the overall function of the CFTR channel. Further functional studies are required to identify the specific site(s) of interaction between the R domain and the NBFs.

Acknowledgements: We thank Drs Junxia Xie and Jiying Zhao for help with the bilayer recordings. We also appreciate critical reading and suggestions of the manuscript by Drs Pamela Davis and Mitchell Drumm. This work was supported by the National Institutes of Health research Grant DK-57710 and an Established Investigator Award from the American Heart Association to J. Ma. B. Zerhusen is a recipient of an NIH predoctoral training Grant (T32HL07714-05).

References

[1] Higgins, C.F. (1992) Annu. Rev. Cell Biol. 8, 67–113.
[2] Riordan, J.R., Rommens, J.M., Kerem, B.-S., Alon, N., Rozmahel, R., Grzelczak, Z., Zielenski, J., Lok, S., Plavsic, N., Chou, J.-L., Drumm, M.L., Iannuzzi, M.C., Collins, F.S. and Tsui, L.-C. (1989) Science 245, 1066–1073.
[3] Picciotto, M.R., Cohn, A.J., Bertuzzi, G., Greengard, P. and Nairn, A.C. (1992) J. Biol. Chem. 267, 12742–12752.
[4] Cheng, S.H., Rich, D.P., Marshall, J., Gregory, R.J., Welsh, M.J. and Smith, A.E. (1991) Cell 66, 1027–1036.
[5] Bear, C.E., Li, C., Kartner, N., Bridges, R.J., Jensen, T.J., Ramjeesingh, M. and Riordan, J.R. (1992) Cell 68, 809–818.
[6] Chang, X.B., Tabcharani, J.A., Hou, Y.X., Jensen, T.J., Kartner, N., Alon, N., Hanrahan, J.W. and Riordan, J.R. (1993) J. Biol. Chem. 268, 11304–11311.
[7] Tabcharani, J.A., Chang, X.B., Riordan, J.R. and Hanrahan, J.W. (1991) Nature 352, 628–631.
[8] Anderson, M.P., Berger, H.A., Rich, D.P., Gregory, R.J., Smith, A.E. and Welsh, M.J. (1991) Cell 67, 775–784.

[9] Hwang, T-C., Nagel, G., Nairn, A.C. and Gadsby, D.C. (1994) Proc. Natl. Acad. Sci. USA 91, 4698–4702.
[10] Rich, D.P., Gregory, R.J., Anderson, M.P., Manavalan, P., Smith, A.E. and Welsh, M.J. (1991) Science 253, 205–207.
[11] Ma, J., Zhao, J., Drumm, M.L., Xie, J. and Davis, P.B. (1997) J. Biol. Chem. 272, 28133–28141.
[12] Winter, M.C. and Welsh, M.J. (1997) Nature 389, 294–296.
[13] Ma, J., Tasch, J., Tao, T., Zhao, J., Xie, J., Drumm, M.L. and Davis, P.B. (1996) J. Biol. Chem. 271, 7351–7356.
[14] Anderson, M.P. and Welsh, M.J. (1992) Science 257, 1701–1704.
[15] Smit, L.S., Wilkinson, D.J., Mansoura, M.K., Collins, F.S. and Dawson, D.C. (1993) Proc. Natl. Acad. Sci. USA 90, 9963–9967.
[16] Carson, M.R., Travis, S.M. and Welsh, M.J. (1995) J. Biol. Chem. 270, 1711–1717.
[17] Sheppard, D.N., Ostedgaard, L.S., Winter, M.C. and Welsh, M.J. (1995) EMBO J. 14, 76.
[18] Gunderson, K.L. and Kopito, R.R. (1995) Cell 82, 231–239.
[19] Drumm, M.L., Wilkinson, D.J., Smit, L.S., Worrell, R.T., Strong, T.V., Frizzell, R.A., Dawson, D.C. and Collins, F.S. (1991) Science 254, 1797–1799.
[20] Xie, J., Drumm, M.L., Ma, J. and Davis, P.B. (1995) J. Biol. Chem. 270, 28084–28096.
[21] Zhao, J., Zerhusen, B., Xie, J., Drumm, M.L., Davis, P.B. and Ma, J. (1996) Biophys. J. 71, 2458–2466.
[22] Zerhusen, B., Zhao, J., Xie, J., Davis, P.B. and Ma, J. (1999) J. Biol. Chem. 274, 7627–7630.
[23] Tao, T., Xie, J., Drumm, M.L., Zhao, J., Davis, P.B. and Ma, J. (1996) Biophys. J. 70, 743–753.
[24] Baukrowitz, T., Hwang, T.C., Nairn, A.C. and Gadsby, D.C. (1994) Neuron 12, 473–482.
[25] Mathews, C.J., Tabcharani, J.A., Chang, X.-B., Jensen, T.J., Riordan, J.R. and Hanrahan, J.W. (1998) J. Physiol. 508, 365–377.
[26] Rich, D.P., Gregory, R.J., Cheng, S.H., Smith, A.E. and Welsh, M.J. (1993) Recept. Channels 1, 221–232.
[27] Ward, C.L. and Kopito, R.R. (1994) J. Biol. Chem. 269, 25710–25718.
[28] Xie, J., Drumm, M.L., Zhao, J., Ma, J. and Davis, P.B. (1996) Biophys. J. 71, 3148–3156.
[29] Pasyk, E.A. and Foskett, J.K. (1995) J. Biol. Chem. 270, 12347–12350.
[30] Dalemans, W., Barbry, P., Champigny, G., Jallat, S., Dott, K., Dreyer, D., Crystal, R.G., Pavirani, A., Lecocq, J.P. and Luzdunski, M. (1991) Nature 4, 526–528.
[31] Li, C., Ramjeesingh, M., Wang, W., Garami, E., Hewryk, M., Lee, D., Rommens, J.M., Galley, K. and Bear, C. (1996) J. Biol. Chem. 271, 28463–28468.
[32] Mathews, C.J., Tabcharani, J.A. and Hanrahan, J.W. (1998) J. Membr. Biol. 163, 55–66.
[33] Wilkinson, D.J., Strong, T.V., Mansoura, M.K., Wood, D.L., Smith, S.S., Collins, F.S. and Dawson, D.C. (1997) Am. J. Physiol. 273, L127–L133.